Vertebrate Anatomy Morphology Palaeontology 10:49–64
ISSN 2292-1389

Consilient evidence affirms expansive stabilizing ligaments in the tyrannosaurid foot

Lara A. Surring[1], Michael E. Burns[2], Eric Snively[3,*], Daniel E. Barta[3], Thomas R. Holtz Jr.[4,5], Anthony P. Russell[6], Lawrence M. Witmer[7], and Philip J. Currie[8]

[1]Alberta Health Services EMS, Calgary, AB, Canada
[2]Department of Biology, Jacksonville State University, Jacksonville, AL, USA
[3]Department of Anatomy & Cell Biology, Oklahoma State University College of Osteopathic Medicine at the Cherokee Nation, Tahlequah, OK, USA; eric.snively@okstate.edu
[4]Department of Geology, University of Maryland, College Park, MD, USA
[5]Department of Paleobiology, National Museum of Natural History, Washington, DC, USA
[6]Department of Biological Sciences, University of Calgary, Calgary, AB, Canada
[7]Department of Biomedical Sciences, Ohio University, Athens, OH, USA
[8]Department of Biological Sciences, University of Alberta, Edmonton, AB, Canada

Abstract: Tyrannosaurid dinosaurs were ecologically unique vertebrates as the sole clade of large terrestrial carnivores (adults >400 kg) in their continent-spanning habitats. Expanded ligaments between metatarsals, inferred by gross morphology of attachment correlates, have been hypothesized to have strengthened their specialized arctometatarsus. We tested the hypothesis of ligament presence with scanning electron microscopy and histological thin sections of putative attachment sites in a third metatarsal of the tyrannosaurid *Gorgosaurus libratus*, compared with a thin section from the unspecialized metatarsals of the early theropod *Coelophysis bauri*. In the *Gorgosaurus* metatarsal, Sharpey´s fibers and rough, pitted surface textures consistent with ligament coalescence occur at expansive distal regions and localized rugosities are ideally located for resisting torsional loading on the foot. Sparser Sharpey's fibers occur at expected locations in other arctometatarsus-bearing coelurosaurs. In contrast, the *Coelophysis* metatarsal lacked Sharpey's fibers or rugosity at the sectioned location, acting as a definitive negative control for identifying these features in tyrannosaurids. With soft-tissue correlates confirmed as ligament entheses, we conclude that tyrannosaurids possessed distinctive and specific ligament attachments to the third metatarsal lacking in other large carnivorous dinosaurs. Histological evidence for extensive distal intermetatarsal ligaments is consistent with greater inferred agility in derived tyrannosaurid dinosaurs than in earlier lineages of large theropods.

INTRODUCTION

Tyrannosaurids were large, ecologically prominent predators with continent-spanning ranges in North America and Asia during the Late Cretaceous (Brusatte et al. 2010). Unusually amongst terrestrial carnivores, adults of later tyrannosaurids were two orders of magnitude more massive than their next-largest adult competitors (Holtz 2002; Snively et al. 2019; Holtz 2021; Schroeder et al. 2021). Success of tyrannosaurids and relatives amongst the larger Tyrannosauroidea has been attributed to unique feeding adaptations, including fused, vaulted nasals (Hurum and Sabath 2003; Rayfield 2004; Snively et al. 2006), a broad skull resistant to torsion and bending (Snively et al. 2006), an expanded secondary palate (Holtz 2002), high bite and neck muscle forces (Snively and Russell 2007a, b; Bates and Falkingham 2012, 2018; Gignac and Erickson 2017; Cost et al. 2019) and robust bone-sundering teeth (Erickson et al. 1996). These adaptations evolved mosaically along the trend to greater adult body size (Erickson et al. 2004; Shychoski 2006; Snively et al. 2006; Li et al. 2010), and reached their greatest extents in *Tyrannosaurus rex*, *Tarbosaurus bataar* and *Zhuchengtyrannus magnus* (Brusatte et al. 2010; Hone et al. 2011), the last and largest tyranno-

Published November 28, 2022
*corresponding author. © 2022 by the authors; submitted June 23, 2022; revisions received September 30, 2021; accepted October 12, 2022. Handling editor: Robert Holmes. DOI 10.18435/vamp29387

saurids. In addition to feeding-related features, postcranial adaptations arising prior to tyrannosaurid diversification, when tyrannosauroids were relatively small (Nesbitt et al. 2019; Zanno et al. 2019), may have catalyzed the group's later ecological exclusivity as large predators (Schroeder et al. 2021; Holtz 2021). For example, derived tyrannosauroids (including tyrannosaurids proper) had anatomical features potentially consistent with greater agility (here defined as the ability to turn more rapidly) than other theropods, such as relatively large leg muscles (Hutchinson et al. 2012; Snively et al. 2019) effective for turning the body, and more compact bodies from nose to tail (Henderson and Snively 2003; Snively et al. 2019) for lower rotational inertia (Carrier et al. 2001; Henderson and Snively 2003; Paul 2005; Snively et al. 2019).

Convergently with other Cretaceous theropods (including ornithomimids, alvarezsaurids, troodontids, and some caenagnathids), tyrannosaurs evolved the arctometatarsalian metatarsus, an elongate and relatively narrow, anteroposteriorly strong metapodium with a proximal splint and distal expansion of the third metatarsal, that conferred capabilities for greater stride length, and higher linear speeds, than was possible in theropods of similar size without such a structure (Holtz 1995, 2001; Snively and Russell 2002, 2003; Snively et al. 2004). Such enhanced ground-covering ability (immediate or long distance: Carrano 1998; Dececchi et al. 2020) would have been valuable whether tyrannosaurids were primarily predators or scavengers. However, the most unusual aspects of arctometatarsus morphology (Fig. 1) offer hints of immediate agility in tyrannosaurs: a wedge-and-buttress constriction of the central third metatarsal (MT III) between the outer bones (Coombs 1978; Holtz 1995), and discrete areas of rugosity on surfaces where the metatarsals articulate with each other distally (Snively and Russell 2002, 2003).

Ligaments hypothesized as emanating from these rugose surfaces would have induced kinematics reinforcing the foot during multi-directional maneuvering (Snively and Russell 2002, 2003). Snively and Russell (2003) established with physical testing that these kinematics would counteract splay at high footfall energies as the central metatarsal (MT III) is displaced anteriorly, and the outer metatarsals are drawn inwards towards the plantar midline of the foot. Other vertebrates put more loading on individual, splaying outer metatarsals, as occurs on the first digit of humans as they quickly accelerate or decelerate laterally during agility tests. In contrast, intermetatarsal kinematics in tyrannosaurids would distribute the loading and therefore forces more evenly amongst the metatarsals, enabling greater forces when maneuvering while maintaining similar stresses (force/area) and tissue safety factors (Snively and Russell 2003). Snively and Russell (2002) established the likely necessity of such ligaments for avoiding breakage of the central metatarsal's proximal splint. These kinematic and structural mechanical hypotheses are subject to refined testing. If the hypotheses are borne out, such ligaments would be consistent with capability for successful prey capture in tyrannosaurids, as with adaptations that similarly enhance agility in predatory animals (Hadziselimovic and Savkovic 1964; Cox and Jeffery 2010; Snively et al. 2019). We refer the reader to these publications for further explication of agility.

Snively and Russell (2003) inferred intermetatarsal ligaments in tyrannosaurids based on gross-scale osteological correlates, but further lines of evidence can test this anatomical inference and form the basis for functional interpretations. We apply scanning electron microscopy and histology to 1) search for finer-scaled correlates of ligament attachment, potentially falsifying the hypothesis that ligaments were present, and 2) to assess whether the direction of ligament insertion is compatible with the splay-negating kinematics that Snively and Russell (2003) proposed. In addition to visually obvious surface rugosity at attachments that are subjected to high loads in life (Snively and Russell 2003, Tumarkin-Deratzian et al. 2007; Petermann and Sander 2013), ligaments and tendons produce microscopic traces of their attachment to bone (Hieronymus 2006; Petermann and Sander 2013) as fibroblasts under tension elongate within the periosteum (Fig. 2), and as parallel osteons form deep to the attachment surface. Ligament entheses also occur within transitional fibrocartilage, which leaves behind a rough bone surface. These histological traces can be used to test hypotheses of ligament presence, differentiating ligament and tendon entheses of attachment from other rough bone surfaces, such as vascularity-striated textures that appear during archosaur growth (Tumarkin-Daratzian et al. 2007; Tumarkin-Daratzian 2009; Brown et al. 2009). Scanning electron microscopy and histological preparations of an adult tyrannosaurid MT III (UALVP 49310) allowed us to assess whether intermetatarsal ligaments were present in a configuration consistent with enhanced tyrannosaur agility.

As a potential control for tyrannosaurid ligament inferences, we examined a metatarsal thin section from the early theropod *Coelophysis bauri* [AMNH FARB 7239], sampled where no gross enthesis correlates are present. The *Coelophysis* histology tests and potentially contradicts the hypothesis of extensive ligaments in tyrannosaurids. Falsifying evidence would include similar correlates in the *Coelophysis* and tyrannosaurid specimens, no microscopic correlates in either, or positive fine-scaled correlates in *Coelophysis* that are absent in the tyrannosaurid metatarsal. Additionally, in light of a previously described histological correlate for ligament attachments (Sharpey's fibers) in the second metatarsal of an alvarezsaur (Qin et al. 2019), we surveyed the literature for similar correlates in other coelurosaurs with arctometatarsalian or subarctometatarsalian (White 2009) pedes to test our predictions about their presence in tyrannosaurids.

MATERIALS & METHODS

Institutional Abbreviations

AMNH FARB, American Museum of Natural History Fossil Amphibians, Reptiles, and Birds collection, New York, New York, USA; BYU, Brigham Young University, Vertebrate Paleontology, Provo, Utah, USA; DINO, Dinosaur National Monument, Jensen, Utah, USA; FMNH, Field Museum of Natural History, Chicago, Illinois, USA; FPDM, Fukui Prefectural Museum, Katsuyama, Fukui, Japan; GI, Geological Institute, Section of Palaeontology and Stratigraphy, Academy of Sciences of the Mongolian People's Republic, Ulaan Bator, Mongolia; HMN, Museum für Naturkunde, Berlin, Germany; IVPP, Institute of Vertebrate Paleontology and Paleoanthropology, Beijing, China; LACM, Natural History Museum of Los

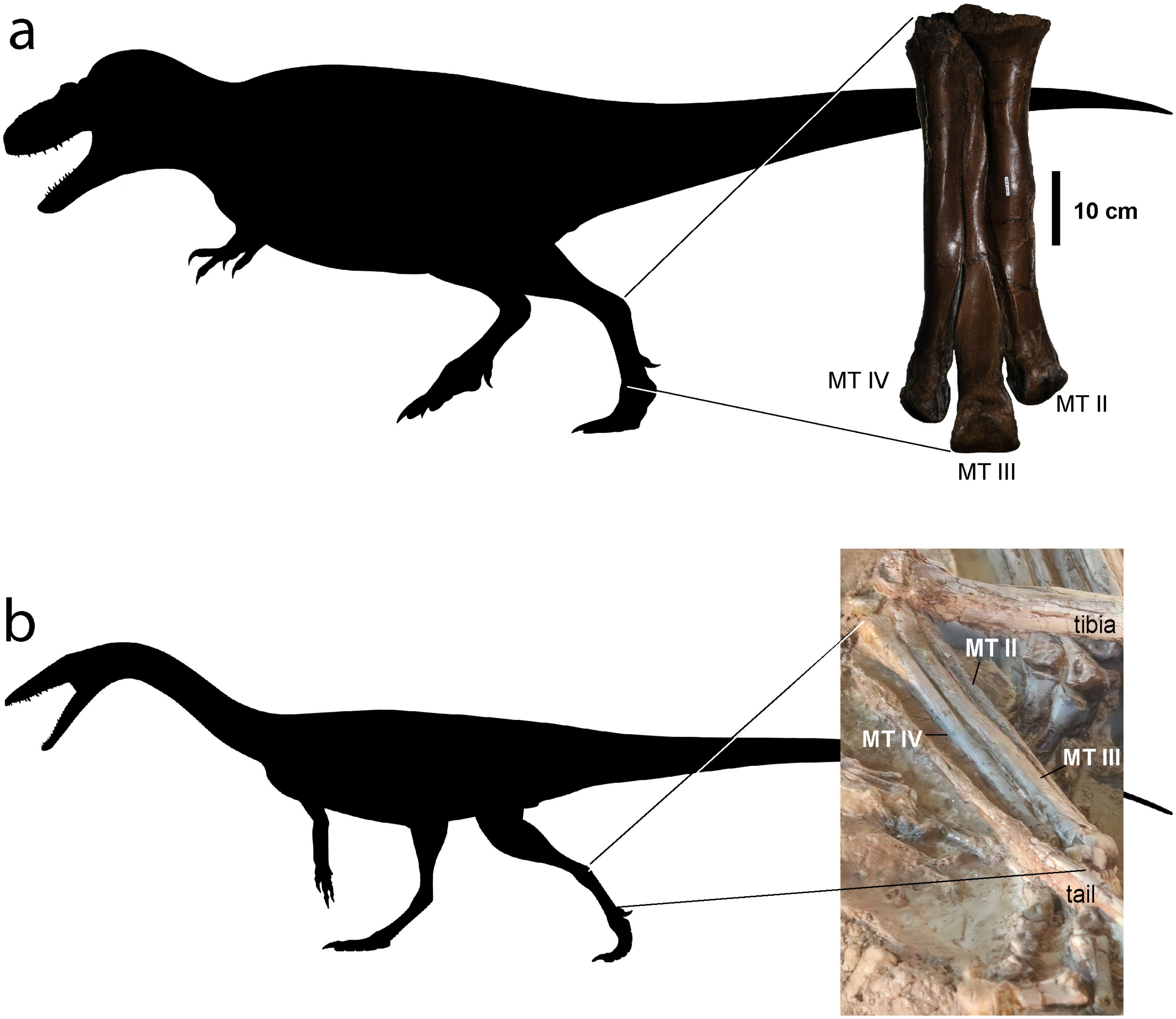

Figure 1. Contrasting morphologies of arctometatarsalian (a) and generalized (b) theropod metatarsals. a, metatarsus of a tyrannosaurid (*Albertosaurus sarcophagus*: TMP 81.10.1) in dorsal view showing proximally constricted MT (metatarsal) III, with plantar constriction evident in ventrolateral slope of the exposed distal MT II articular surface with MT III; b, metatarsus of *Coelophysis bauri* (LACM 153347 block) in dorsoolateral view, showing proximally broad, anteriorly positioned MT III, unlike the interpretation depicted in Colbert (1989). Silhouette of *Gorgosaurus libratus* by Matthew Dempsey and silhouette of *Coelophysis bauri* by Scott Hartman, both available from Phylopic under a CC BY 3.0 license (https://creativecommons.org/licenses/by/3.0/).

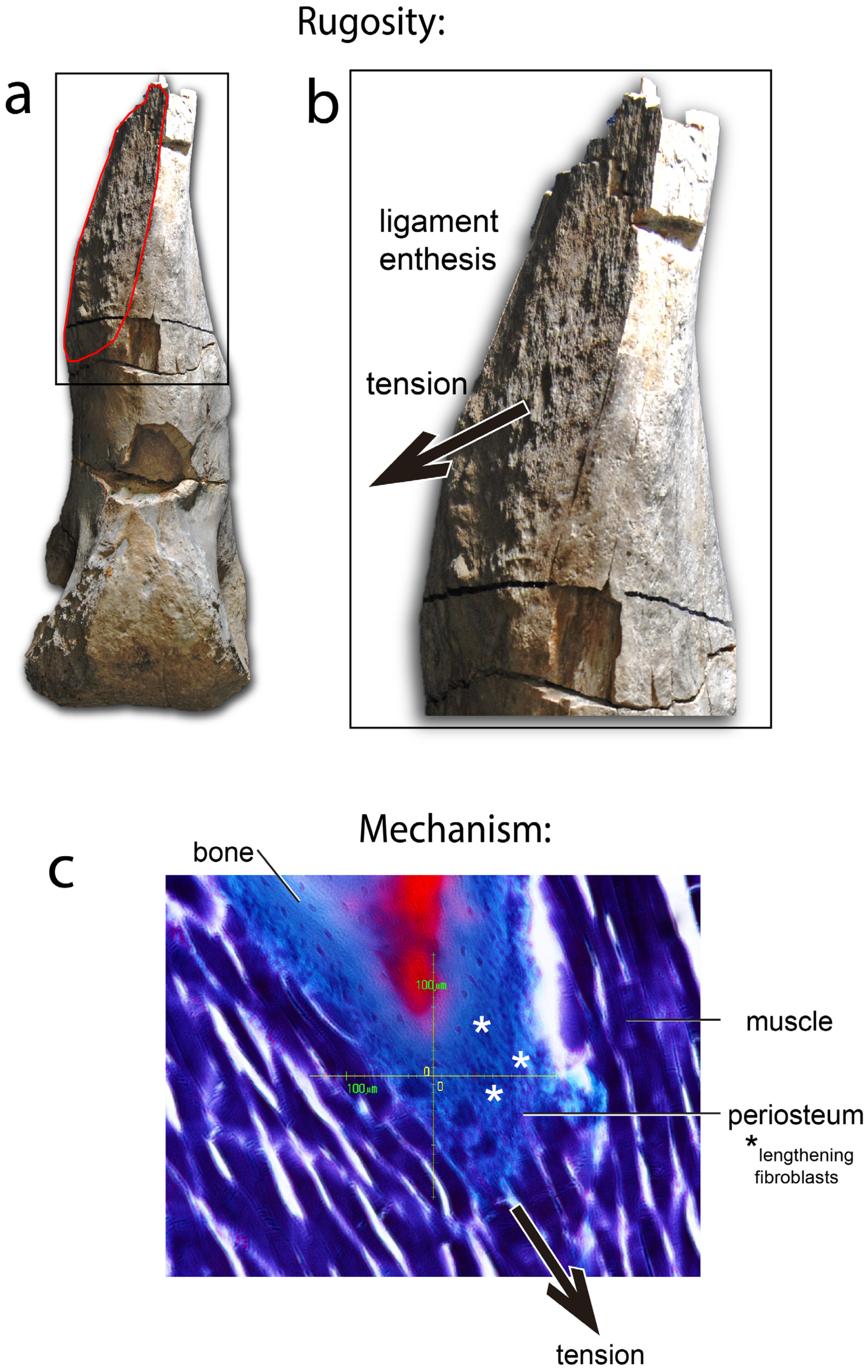

Figure 2. a–b, Gross morphology of hypothesized ligament attachments; a, *Gorgosaurus libratus* (UALVP 49310) Metatarsal III (MT III), distal end. Outline around distal portion of large surface for articulation with MT II; b, close-up with low-angle light relative to MT II articular surface, showing rugosity indicative of a ligamentous enthesis. Arrow illustrates tension on enthesis, inferred as causing the rugosity; c, mechanism underlying enthesis rugosity in the femur of the lacertid lizard *Podarcis hispanicus* (H77, Collection of the Biology Department, Autonomous University of Madrid, Spain). Elongation of fibroblasts (*) under tension (muscular in this case) produces parallel bundles of collagen fibers at muscle and ligament attachments.

Angeles County, Los Angeles, USA; MOR, Museum of the Rockies, Bozeman, Montana, USA; MWC, Museum of Western Colorado, Fruita, Colorado, USA; NIGP, Nanjing Institute of Geology and Palaeontology, Academia Sincia, Nanjing, China; NMC Canadian Museum of Nature collections, Gatineau, Quebec, Canada; NMMNH, New Mexico Museum of Natural History and Science, Albuquerque, New Mexico, USA; OMNH, Sam Noble Museum of Natural History, Norman, Oklahoma, USA; PVL, Paleontologia de Vertebrados Lillo, Universidad Nacional de Tucuman, Tucman, Argentina; PVPH, Museo Carmen Funes, Paleontología de Vertebrados, Plaza Huincul, Neuquén Province, Argentina; ROM, Royal Ontario Museum, Toronto, Ontario, Canada; TMP, Royal Tyrrell Museum of Palaeontology, Drumheller, Alberta, Canada; UALVP, University of Alberta Laboratory for Vertebrate Palaeontology, Edmonton, Alberta, Canada; UMNH, Utah Museum of Natural History, Salt Lake City, Utah, USA; YPM, Yale Peabody Museum, New Haven, Connecticut, USA.

Methods

We reviewed macrocsopic correlates for ligamentous attachments in comparative specimens that Snively et al. (2004) examined, with the addition of many recently-collected tyrannosaurid metatarsals at UALVP and TMP (Tab. 1). We also surveyed the literature for descriptions of histological correlates in additional coelurosaurian metatarsals. One tyrannosaurid specimen, UALVP 49310, was selected for paleohistological analysis. This specimen is a distal portion of metatarsal III of *Gorgosaurus libratus* collected from the Upper Campanian (Upper Cretaceous) Dinosaur Park Formation in Dinosaur Provincial Park, Alberta, Canada. Arctometatarsalian third metatarsals (MT III) are triangle-shaped in distal cross-sections (Holtz 1995), with a posterior constriction that forms a ridge (also called a plantar constriction; Snively et al. 2004). UALVP 49310 is identifiable as *Gorgosaurus* MT III by its curving, distally extended posterior constriction., differing from the contemporaneous *Daspletosaurus* which has a straighter, broader, oblong, and less edge-like constriction distally (Yun 2021).

Paleohistological analysis was conducted by cutting thin sections transversely through the entire diaphysis of the metatarsal (Fig. 3a, b). The section was initiated at the most protuberant region of the central rugosity on the lateral surface (attachment site for the metatarsal III-IV ligament). One-centimeter-diameter cores were also cut from the bone and divided sagittally to permit mounting on slides. The samples were stabilized via resin impregnation using Buehler EpoThin Low Viscosity Resin and Hardener prior

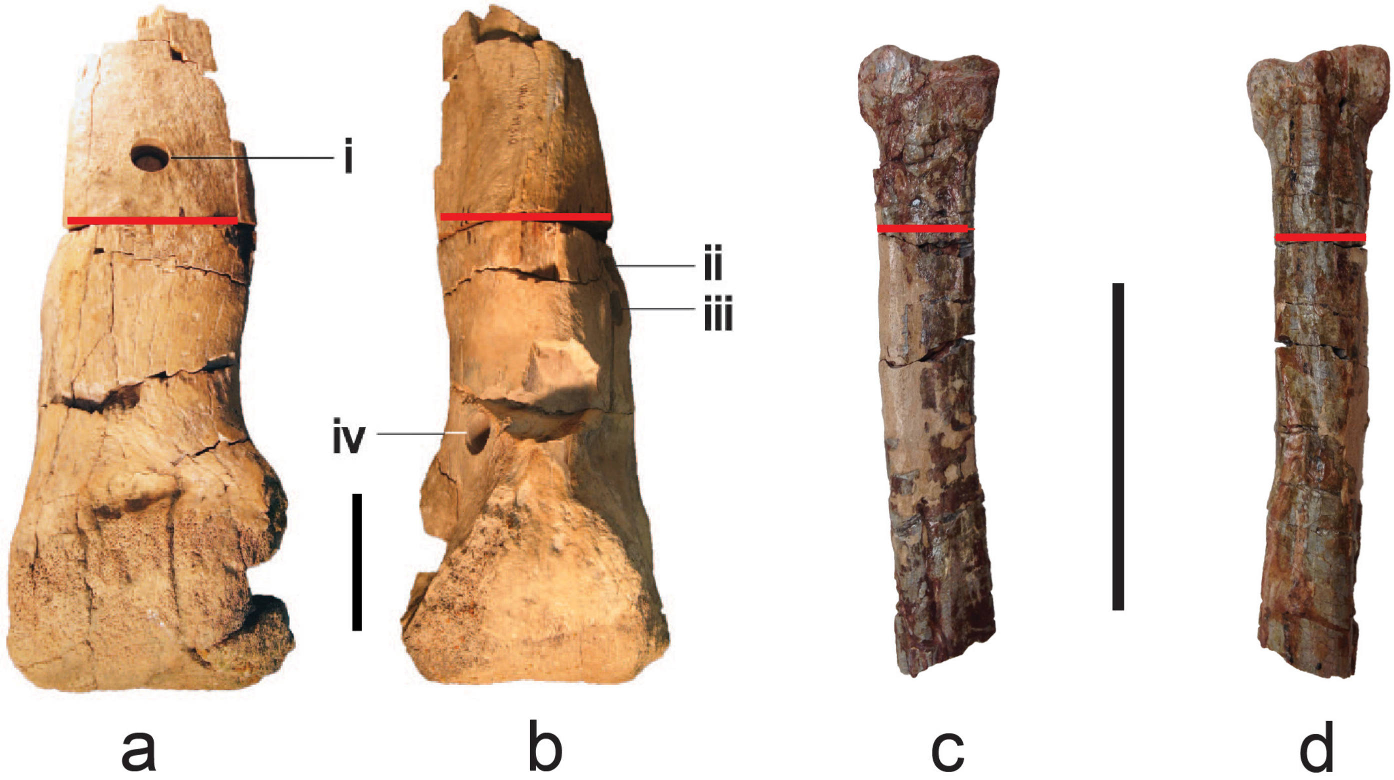

Figure 3. a, b, distal portion of adult *Gorgosaurus libratus* (UALVP 49310) third metatarsal (right), in a, dorsal and b, ventral views, showing locations of whole-bone transverse section (transverse line) and histological core samples (i-iv). Core iv is from a smooth-surfaced scalloped area. Scale bar = 5 cm; c, d, Proximal portion of *Coelophysis bauri* (AMNH FARB 7239) third metatarsal (right) in lateral (c) and medial (d) views, showing location of whole-bone transverse section. Scale bar = 5 cm.

Table 1. Theropod metatarsal specimens examined. Ontogenetic stage is inferred based on striated (juvenile) or smooth (adult) subcutaneous bone texture, or assessments from original descriptions.

Taxon	Specimen number	Ontogenetic stage
Albertosaurus sarcophagus	AMNH 5432	Adult
Albertosaurus sarcophagus	TMP 1999.050.0025	Subadult
Albertosaurus sarcophagus	TMP 1981.010.0001	Adult
Albertosaurus sarcophagus	TMP 1986.064.0001	Juvenile-subadult
Albertosaurus sarcophagus	TMP 1999.050.0012	Juvenile
Albertosaurus sarcophagus	TMP 1988.016.0022	Subadult-adult
Allosaurus jimmadseni	MOR 693	Adult
Allosaurus fragilis	ROM 5091	Adult
Allosaurus jimmadseni	DINO 11541	Subadult-adult
Allosaurus maximus	OMNH 01708	Adult
Bambiraptor feinbergi	AMNH 30556	Subadult
Carcharodontosauridae	PVPH 108-31	Adult
Chirostenotes pergracilis	NMC 8538	Adult
Coelophysis bauri	TMP block	Adult
Daspletosaurus sp.	TMP 2001.036.0001	Subadult-adult
Daspletosaurus sp. or *Gorgosaurus libratus*	TMP 1994.172.0099	Juvenile
Daspletosaurus sp. or *Gorgosaurus libratus*	TMP 1999.055.0113	Subadult-adult
Daspletosaurus sp. or *Gorgosaurus libratus*	TMP 1968.003.0001	Adult
Deinonychus antirrhopus	MOR 947	Adult
Deinonychus antirrhopus	YPM 5205	Adult
Elaphrosaurus bambergi	HMN Gr.S. 38–44	Adult
Elmisaurus sp.	TMP/PJC, photographs	Adult
Fukuiraptor kitadaniensis	FPDM V9712224	Subadult-adult
Gorgosaurus libratus	TMP 1994.012.0602	Adult
Gorgosaurus libratus	TMP 1979.014.0704	Adult
Gorgosaurus libratus	TMP 1967.014.0022	Juvenile
Gorgosaurus libratus	TMP 1986.144.0001	Juvenile
Gorgosaurus libratus	TMP 1991.036.0500	Juvenile-subadult
Gorgosaurus libratus	TMP 1981.039.0021	Adult
Gorgosaurus libratus	TMP 1973.030.0001	Adult
Gorgosaurus libratus	TMP 1967.010.0041	Juvenile
Gorgosaurus libratus	UALVP 10	Adult
Gorgosaurus libratus	UALVP 49310	Subadult-adult
Herrerasaurus ischigualestensis	PVL 2566	Adult
Ingenia yanshini	GI 100/34	Adult
Ingenia yanshini	GI 100/32	Adult
Ornitholestes hermanni	AMNH 619	Adult

Table 1 continued.

Ornithomimidae	TMP 1987.054.0001	Subadult/adult
Rinchenia mongoliensis	GI 100/42	Adult
Segnosaurus ghalbinensis	GI SPS 100182	Adult
Sinosauropteryx prima	NIGP 127587	Adult
Sinraptor dongi	IVPP 10600	Adult
Tarbosaurus bataar	PIN 552-1	Adult
Tanycolagreus topwilsoni	TPII 2000-09-29	Adult
Torvosaurus tanneri	BYU 7255277	Adult
Torvosaurus tanneri	BYU 7255280	Adult
Troodon formosus	MOR 493	Adult
Troodon formosus	TMP 1991.026.0575	Adult
Tyrannosaurus rex	FMNH PR 2081	Adult
Tyrannosaurus rex	LACM 7244/23844	Adult
Tyrannosaurus rex	MOR 555	Adult
Tyrannosaurus rex	TMP 1981.006.0001	Adult
Tyrannosaurus rex	TMP 1981.012.0001	Adult

to sectioning. Cutting and grinding followed procedures for standard petrographic sections. Sections were ground to a thickness of 60–80 μm (measured using interference colors), depending on the visibility of internal structures of interest. The sections were examined using a Nikon ECLIPSE E400 POL Polarizing Microscope in plane polarized (PPL) and cross-polarized (XPL) light.

Scanning electron microscopy was performed to image the surface texture of the four cores used for histologic analysis (Fig. 3a, b). The cores were coated with approximately 100 Ångstroms of gold and examined using a JEOL 6301 FE scanning electron microscope. The accelerating voltage was 5.0 kv and the working distance was 15 mm.

A *Coelophysis bauri* metatarsal, AMNH FARB 7239, was previously sectioned by one of us (DEB) for display in the 2016-2017 AMNH Dinosaurs Among Us special exhibition and proved useful for comparison in the current study. We identified it as a right metatarsal III based on the presence of articular facets on two sides, a large anterior tuberosity, a laterally offset proximal depression for a distal tarsal, and a sharp ventral constriction between the expanded proximal end and the diaphysis (Fig. 3c, d). Though unfused to metatarsal II, unlike the fused condition in some *C. bauri* (e.g., NMMNH P-42200) (Rinehart et al. 2009, fig. 80A, D), the element nevertheless shares these similarities with the third metatarsal of NMMNH P-42200 and those of the coelophysoids '*Syntarsus*' *kayentakatae* and *Powellvenator podocitus* (Tykoski 2005:fig. 102C, E; Ezcurra 2017:fig. 9). AMNH FARB 7239 was sectioned transversely across its entire diaphysis, near the proximal end (Fig. 3c, d). The sampled fragment was embedded in epoxy, sectioned with a Buehler Isomet 11-1180 low speed saw, ground until optically transparent and imaged with a Nikon Optiphot 2 petrographic microscope in plane polarized (PPL) and cross-polarized (XPL) light.

RESULTS

The proximal portions of the tyrannosaurid MT III examined in this study exhibit large ligament scars similar to those previously reported in other theropod specimens. Unlike other large theropods however, tyrannosaurid MT III bear enormous, rugose ovoid facets distally along MT III-IV and MT II-III articular surfaces (Fig. 4a) as reported by Snively and Russell (2003).

Other features flank this scar distally, or contribute to its topography. A regularly-oriented, oblong tuberous ridge (the primary tuberosity) occurs along the anterior border of the large, distal scar in tyrannosaurids regardless of individual age and taxonomic variation. The extent of rugose surface texture related to the primary tuberosity appears age-dependent, and is typically less developed and covers less surface area in smaller tyrannosaurid MT III interpreted as juveniles (Tab. 1). A smooth scalloped area is noticeable distal to the primary tuberosity and dorsal to the posterior collateral ligament pit, but the overall size and depth of the scalloped surface is expressed to a lesser degree in *Tyrannosaurus rex* than in other tyrannosaurids.

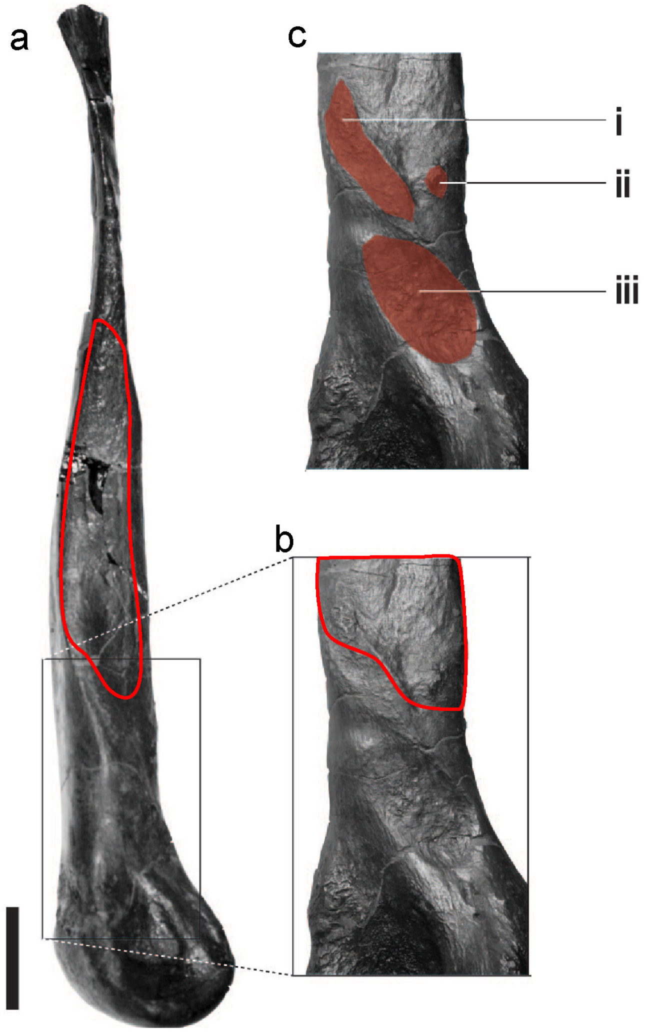

← **Figure 4.** a, Adult *Gorgosaurus libratus* (UALVP 10) left MT III, distal portion, lateral view. The proximal 18% of the element is missing. The red outline traces the full, rugose distal surface of articulation with MT IV; b, inset box highlights a broad region of rugosity for attachment of the MT III–IV ligament; c, more distal attachments of the MT III–IV ligaments, including the primary tuberosity (i); accessory tuberosity (ii); scalloped region and secondary tuberosity (iii). Scale bar = 5 cm. The Roman numerals here do not correspond with those in Figures 3 and 6.

In observed specimens of albertosaurine tyrannosaurids (*Gorgosaurus libratus* and *Albertosaurus sarcophagus*), a secondary tuberosity commonly accompanies the posterior border of the scallop and all juvenile tyrannosaurids show deeper scalloping with clearly demarcated borders. A smaller, circular, accessory tuberosity, frequently found near the posterior base of the primary tuberosity (Fig. 4c), is exaggerated in specimens of *Tyrannosaurus rex*.

Parallel, linear assemblages of microscopic fibrocartilaginous ligament-bundle insertion pits (individual 'entheses', Shaw and Benjamin 2007) align with the long axis of each tuberosity (Figs. 5, 6). Scanning electron microscopy reveals distinct differences in surface texture, enthesis pit morphology and distribution between regions that relate to the extent of ligament involvement (Fig. 6). The deepest pits, as well as the majority of pits, are found immediately bordering the tuberosities. No pitting is observed where ligaments are not predicted to attach (Fig. 6d).

The outermost cortex of three of the four core samples is characterized by periosteal bone. Sharpey's fibers reveal that ligaments penetrated the periosteal surface at angles of 20–50°, although their direction relative to the periosteal surface is consistent within each core (Fig. 7). At the roughest surfaces (Fig. 7b, c), Sharpey's fibers are multidirectionally angled relative to the bone surface, as common in strong entheses (Apostolakos et al. 2014). Sharpey's fibers occur with consistent direction at the external surface and deep to lines of arrested growth when LAGs are evident in the thin section, as seen in extant *Alligator* (Petermann and Sander 2013).

In addition, the enthesis histology directly resembles that occurring at smaller ligament and tendon attachments in *Alligator* (Hieronymus 2006; Tumarkin-Deratzian et al.

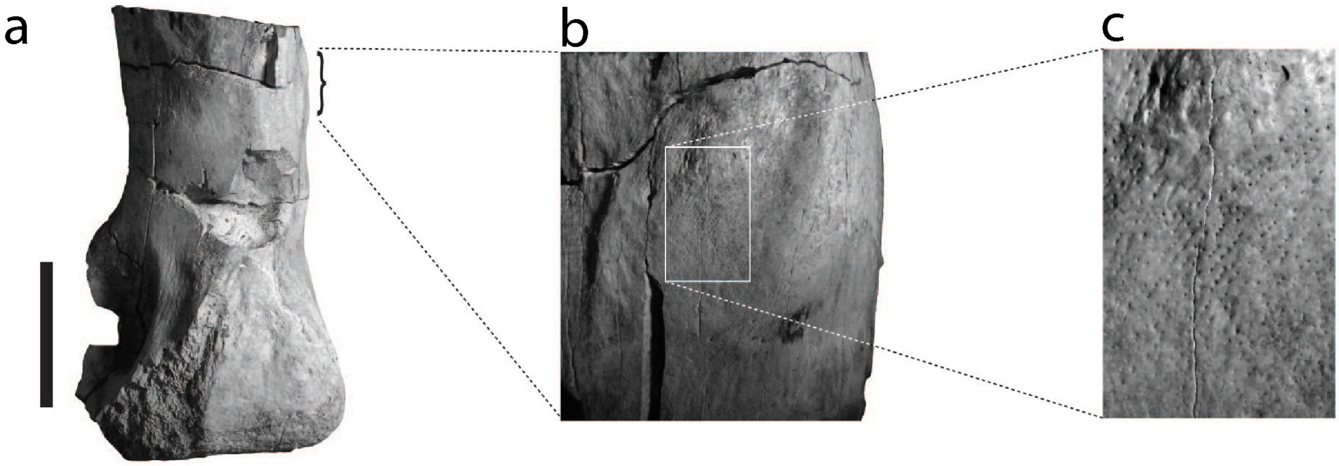

Figure 5. Adult *Gorgosaurus libratus* (UALVP 49210) distal right MT III, partial ventral view. Bracket and insets highlight the primary tuberosity and individual ligament pits, which form oblique linear assemblages. Scale bar = 5 cm.

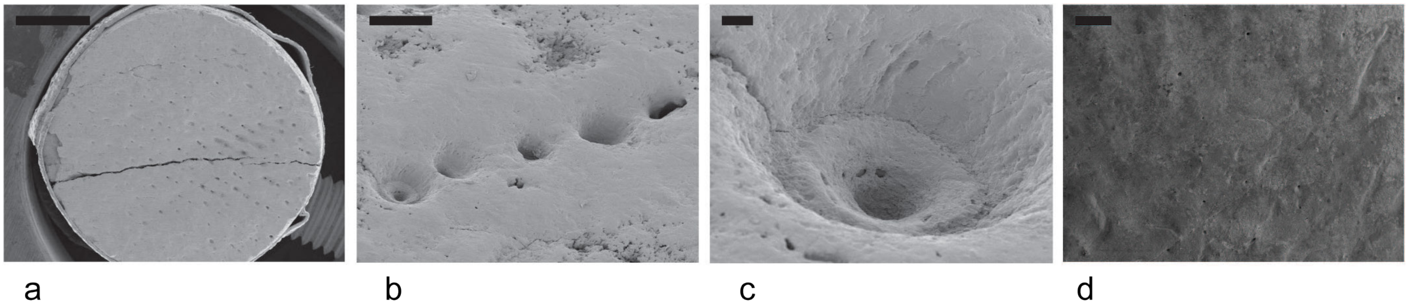

Figure 6. a, scanning electron micrographs (SEM) of *Gorgosaurus libratus* (UALVP 49310) core sample iii showing linear, parallel assemblages of ligament pits, scale bar = 2.5 mm; b, SEM detail of linearly-arranged ligament pits, scale bar = 250 µm; c, SEM of isolated ligament pit, scale bar = 25µm; d, Contrasting SEM of core sample iv (Fig. 4) showing non-ligamentous surface (scale bar = 250 µm.

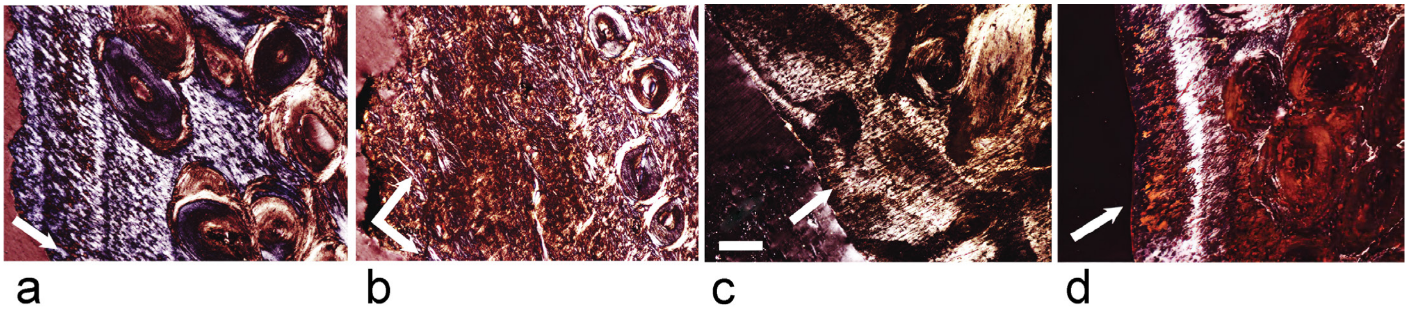

Figure 7. a, histological sections from *Gorgosaurus libratus* (UALVP 49310) MT III core sample i, Sharpey's fibers (white arrow) insert are parallel, consistent with a tight periosteum; b, Core histology for sample ii (primary tuberosity with ligament pits); multi-directional Sharpey's fibers correspond to superficial rugosity, consistent with anchoring function of ligament attachment; c, Core histology for sample iii (primary tuberosity with ligament pits), Sharpey's fibers inserting irregularly into bone surface (intermediate between a and b); d. Core histology for sample iv (non-ligamentous bone surface), which is depauperate of Sharpey's fibers. All histological sections viewed under cross-polarized light with periosteal (superficial) surface to the left of each panel. Scale bar = 1 mm.

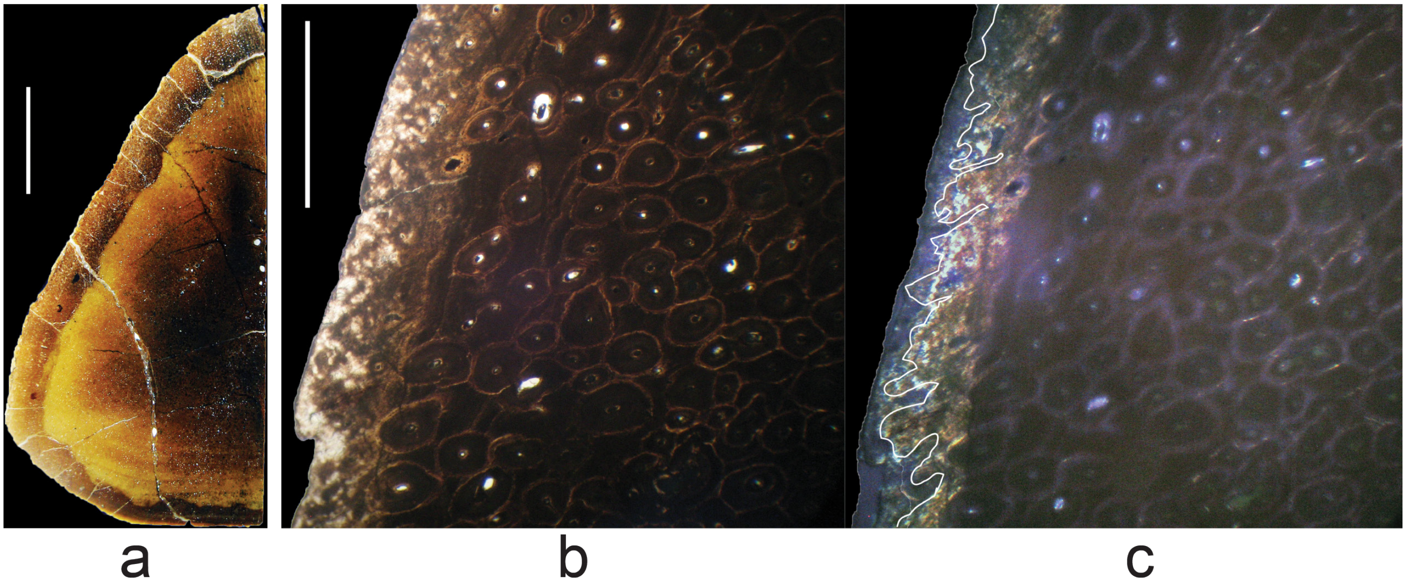

Figure 8. a, Right side of entire section through the entire MT III of *Gorgosaurus libratus* (UALVP 49310) at the location indicated in Figure 3. Dorsal is towards the bottom. Scale bar = 1 cm; b, c, insets with different polarizing filters show undulations characteristic of fibrocartilaginous ligament entheses (Tumarkin-Deratzian et al. 2007; Apostolakos et al. 2014), outlined in c. Scale bar = 2 mm.

2007) in which an undulating subperiosteal structure is evident in thin section (Fig. 8), and differs from the histology of other rough bone surfaces in that taxon (Tumarkin-Deratzian et al. 2007). Furthermore, Sharpey's fibers in the *Gorgosaurus* MT III resemble those at femoral muscle attachments in *Alligator mississippiensis*, the rabbit *Oryctolagus cuniculus*, and turkey *Meleagris gallopavo* (Petermann and Sander 2013), but in *Gorgosaurus* are consolidated into more robust bundles than in these smaller tetrapods. The enthesis histology and pitting occurs across both expansive and localized attachment sites (Figs. 4, 5) in the tyrannosaurid metatarsal, indicating great cross-sectional areas of ligaments with high aggregate stiffness and strength. The dorsal side of the *Coelophysis bauri* proximal metatarsal III (AMNH FARB 7239) lacks Sharpey's fibers and comprises largely woven bone surrounding primary osteons lined by lamellar bone (Fig. 9). The vasculature is primarily reticular to longitudinal, with some vascular spaces forming large cavities at this plane of section. An inner circumferential layer of lamellar bone lines the medullary surface. The outermost cortex shows greatly reduced vascularity, and may consist of parallel-fibered bone, despite being somewhat opaque, likely reflecting diagenetic alteration and/or increased thin section thickness towards the periosteum. Nevertheless, no Sharpey's fibers are seen anywhere in the section.

DISCUSSION

Ligament Inferences in the Context of Theropod Metatarsal Histology

Correlates suggestive of distal intermetatarsal ligaments in tyrannosaurids are not present in their extant bracket (birds and crocodylians, Witmer 1995). Characterizing these soft tissues therefore requires high-order inference (Bryant and Russell 1992; Witmer 1995) and additional lines of evidence, such as our comparative SEM and bone histology. These methods enable microscopic assessment of soft-tissue traces universal amongst vertebrates, such as Sharpey's fibers evident in ground thin sections.

Our inferences of ligamentous soft tissues in *Gorgosaurus* at the sampled locations are consistent with histological evidence for Sharpey's fibers in other theropods. The histology of the proximal portion of metatarsal III of both *Coelophysis bauri* and the coelophysoid *Powellvenator* (Ezcurra 2017) reveals no evidence of Sharpey's fibers. Therefore, we can state that Sharpey's fibers are not ubiquitously distributed throughout individual metatarsals of these early diverging theropods, which fails to falsify our hypothesis that Sharpey's fibers are only concentrated at localized ligamentous attachment sites. We predict that further sampling will show that the distal portions of early diverging theropod metatarsals also lack Sharpey's fibers consistent with ligament attachment, in contrast with our finding of distal Shapey's fibers in *Gorgosaurus*. Non-tyrannosauroid coelurosaurs, including maniraptorans, provide further data for comparison. Sharpey's fibers do not appear present in the subarctometatarsalian metatarsals of troodontids sectioned to date (Varricchio 1993; Erickson et al. 2007; Sellés et al. 2021), nor have they been reported from midshaft thin sections of ornithomimosaur fourth metatarsals (Watanabe et al. 2013; Cullen et al. 2014). To date the only published, histologically confirmed occurrence of Sharpey's fibers in a theropod metatarsal are those of the distal end of metatarsal II of *Xixianykus zhangi*, an alvarezsaur which also has an arctometatarsalian pes (Qin et al. 2019). Additionally, the elmisaurine oviraptorosaur *Leptorhynchos elegans* appears to have sparsely distributed Sharpey's fibers along the periosteal surface of the anteromedial corner of metatarsal III (Funston et al. 2016:fig. 9G) deep to its surface of articulation with metatarsal II. This position is consistent with predicted ligamentous entheses in arctometatarsalian pedes and concurs with our observation of localized Sharpey's fibers at ligamentous attachments in tyrannosaurids.

Function of Tyrannosaurid Arctometatarsus Ligaments

As in extant vertebrates, ligament surface pitting and Sharpey's fibers in the *Gorgosaurus* metatarsal are inferred to have arisen from a mechanobiologic process relating directly to stress transfer at the ligament-bone junction (Fig. 2; Carter and Beaupré 2001). Why are these entheses particularly extensive and robust in the arctometatarsus of tyrannosaurids, and what selective factors shaped their likely adaptive roles? As proposed in the Introduction, we posit that the confirmed ligaments played a direct role in locomotor agility in long-footed tyrannosaurids.

Distal regions of the limbs of large, extant vertebrates routinely experience complex loads and can fail when overloaded during fast, agile locomotion, as seen in horses (Ely et al. 2009). Attempted maneuvering at larger body sizes imposes greater torsional loadings that critically stress specific regions of the skeleton unless changes in size, shape, material properties and/or function occur to accommodate these loads; these adaptive allometries become more prominent as body mass exceeds 300 kg (Biewener 2005). Consistent with relatively compact body proportions and large leg muscles suggestive of enhanced agility in tyrannosaurids (Snively et al. 2019), the arctometatarsus displays architectural (Wilson and Currie 1985; Holtz 1995; Snively and Russell 2003) and ligamentous modifications (Snively and Russell 2002, 2003; current study) that can be deduced from the macro- and microscopic soft-tissue traces that remain.

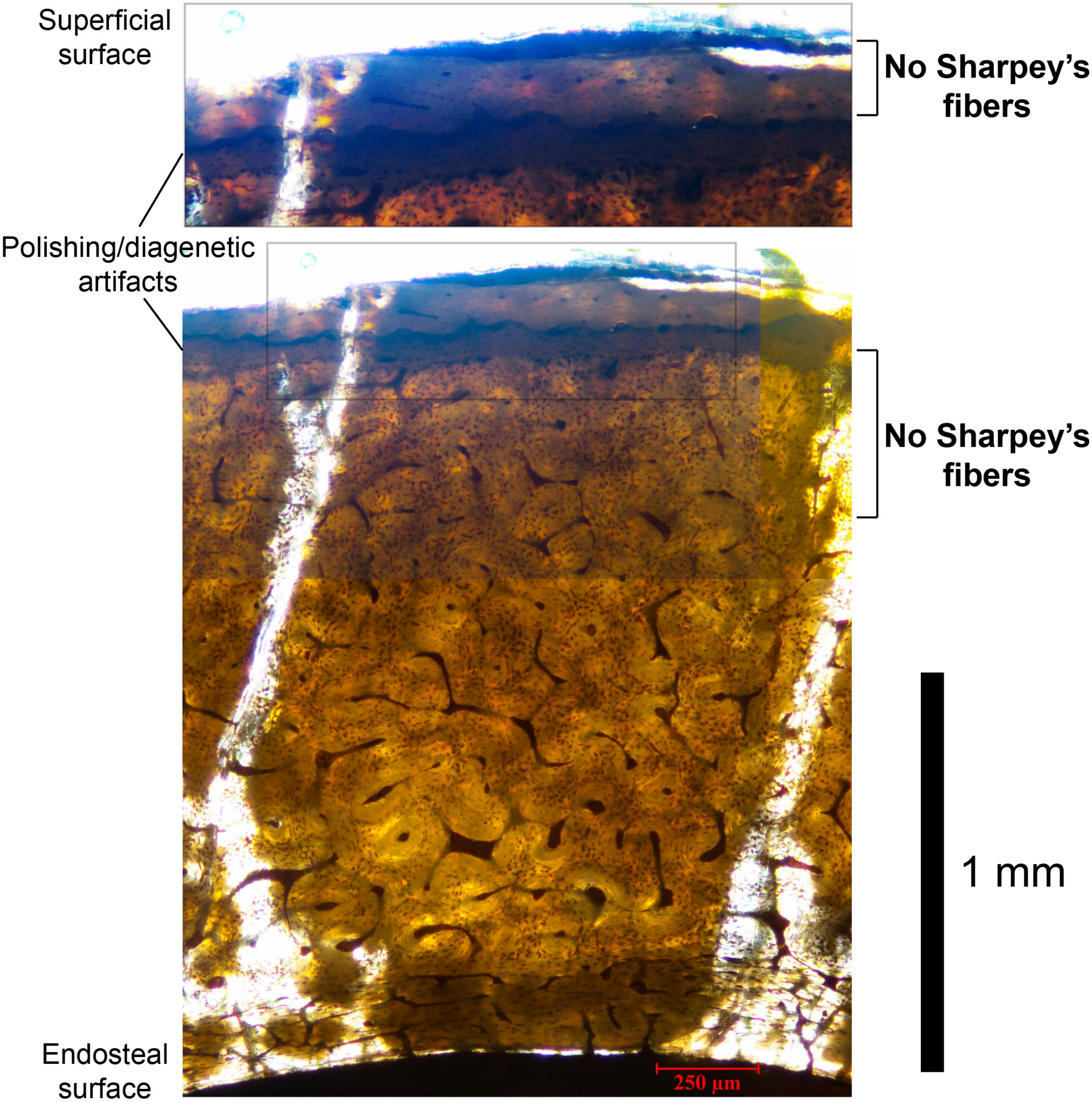

Figure 9. Thin section through anterior cortex of *Coelophysis bauri* metatarsal III (AMNH FARB 7239), at the location in Figure 3. The lower image depicts the section traversing from endosteal to periosteal surfaces, and the upper image is modified to better show osteocyte lacunae. No Sharpey's fibers or other enthesis correlates are present that would indicate ligament attachment, in contrast with the *Gorgosaurus libratus* MT III sections (Figs. 7, 8). A "Dehaze" filter was applied to the lower figure to compensate for opacity of its superficial portion (see text).

We interpret the ligament attachment correlates with the maintenance of agile maneuvers, for which regions of calcified ligamentous attachments are effective at withstanding greater stresses at the ligament-bone interface (Shaw and Benjamin 2007). Parallel assemblages of microscopic entheses would have permitted local transduction of foot compressive forces to tension with a tensegrity-style mechanism (Snively and Russell 2003; Sellers et al. 2017). Collectively these large ligament attachments would have distributed regional tensile stresses to enhance strength in the tyrannosaurid foot (Shaw and Benjamin 2007). The expanded extent of the distal scar that approached the collateral ligament pits indicates reinforcement of the tyrannosaurid limb to a greater extent than that conferred by the ligaments of other theropods. This is especially true for adult *Tyrannosaurus rex*, in which the scars are further expanded proximally to capture greater relative surface areas (Snively and Russell 2003). The three distinctly oriented tuberosities furnish even greater surface area as ligament anchors, thereby enhancing the effectiveness of the ligaments by transferring regional torsional stresses to minimize intermetatarsal splay (lateral spreading of the bones from each other, Snively and Russell 2003). These distal attachments are not present in allosauroids similar in size to adult *Tyrannosaurus* (Snively et al. 2004), including *Mapusaurus*, *Acrocanthosaurus*, and an examined large carcharodontosaurid (PVPH 108-31). Relatively large ligaments in adult *T. rex* are, therefore, not solely attributable to weight bearing, and as in its smaller relatives likely assisted in high maneuverability relative to body size (Snively et al. 2019).

Synthesis 1: Musculoskeletal Evidence of Tyrannosaurid Agility is Consistent with Semicircular Canal Morphology

Expansive foot ligaments and dynamics calculations (Snively et al. 2019) suggest competent agility in tyrannosaurids that is consistent with their neurosensory morphology. The semicircular canals of tyrannosaurids are expanded, especially the lateral canal (e.g., *Tyrannosaurus* CMNH 7541, AMNH FR 5117) versus other large theropods (*Allosaurus* UMNH VP18050, *Ceratosaurus* MWC 1.1, Witmer and Ridgely 2009; Sampson and Witmer 2007). This expansion suggests the capability for enhanced vestibulo-ocular and vestibulocollic reflexes important for tracking and striking prey (Witmer et al. 2008; Witmer and Ridgely 2009; Bronzatti et al. 2021).

The inner ear structure of mammals, birds, and large dinosaurs has been broadly linked to locomotor agility based on the sizes and shapes of the semicircular canals (Hadziselimovic and Savkovic 1964; Money et al. 1974; Spoor et al. 2007; Cox and Jeffery 2010) and their neural connections with the visual system to stabilize gaze. Although quantitative studies of comparable scope to those done for mammals have not been done for dinosaurs, the finding that canals are relatively elongate in agile mammals (such as cheetahs and bats, Cox and Jeffery 2010, brachiating primates, Spoor et al. 2007; Cox and Jeffery 2010) and birds (Hadziselimovic and Savkovic 1964) is fully consistent with our evidence for rapid maneuvers in tyrannosaurids. As in other small coelurosaurs, juvenile tyrannosaurids would benefit more from synapomorphically large canals (Witmer and Ridgely 2009) for full-body maneuvers than would slower reacting, slower turning tyrannosaurid adults (More et al. 2010, Snively et al. 2019). Once in range, tyrannosaurid adults could engage vestibular reflexes for rapid and controlled head-neck movements (Snively and Russell 2007; Witmer and Ridgely 2009).

Synthesis 2: Ecological and Evolutionary Implications of Tyrannosaurid Agility

Whereas tyrannosaurids were the only large carnivorous dinosaurs in latest Cretaceous (Campanian and Maastrichtian) terrestrial communities of Asia and North America (Fig. 10), earlier dinosaur-dominated ecosystems typically had representatives of various theropod clades (ceratosaurs, megalosauroids, allosauroids, and various coelurosaur groups) separately occupying different adult size classes (Fig. 10; Farlow and Holtz 2002; Holtz 2004; Schroeder et al. 2021; Holtz 2021). The Tyrannosauroidea, the more inclusive clade of which the giant Tyrannosauridae are the last, largest, and most derived (Holtz 2004, Brusatte et al. 2010), was present from the Middle Jurassic onward (Brusatte et al. 2010), are represented by small- and medium-sized components of these diverse assemblages (Nesbitt et al. 2019; Zanno et al. 2019). At present, there is little direct evidence to determine whether the transition from ecosystems of numerous large theropod families to those dominated by tyrannosaurids is reflective of competitive displacement, or decline and opportunism. Regardless of the scenario, the modifications of the arctometatarsus that permitted greater agility evolved initially in the context of smaller body size (Nesbitt et al. 2019; Zanno et al. 2019) and became effective even in the largest individuals of the derived forms. The unique tyrannosaurid arctometatarsus would have enhanced the tyrant dinosaurs' potential in prey acquisition.

ACKNOWLEDGEMENTS

Particular thanks to Morgan Turner for an essential review of this manuscript. We thank Denver Fowler and anonymous reviewers for comments on previous versions. We recognize the University of Alberta Earth and Atmospheric Sciences Laboratory for thin-sections (Mark Labbe), the Scanning Electromicroscopy Laboratory (George Braybrook and Martin Kupsta), the Palaeontology Micro Computed Tomography Laboratory (Alison Murray) and the Botany Thin-sectioning Laboratory (Ruth Stockey). Thanks to Phil Bell for the discovery of UALVP 49310 and University of Alberta Laboratory of Vertebrate Palaeontology collections for permission to use the specimen in consumptive analyses. The Royal Tyrrell Museum of Palaeontology provided research space (Don Brinkman), specimen loans and photographs of UALVP 10 (Brandon Strilisky, Tom Courtney, Kari Leiper, and Martin Schilling), and enlightening discussion (Darren Tanke and Michael Newbrey). For collections access and permission

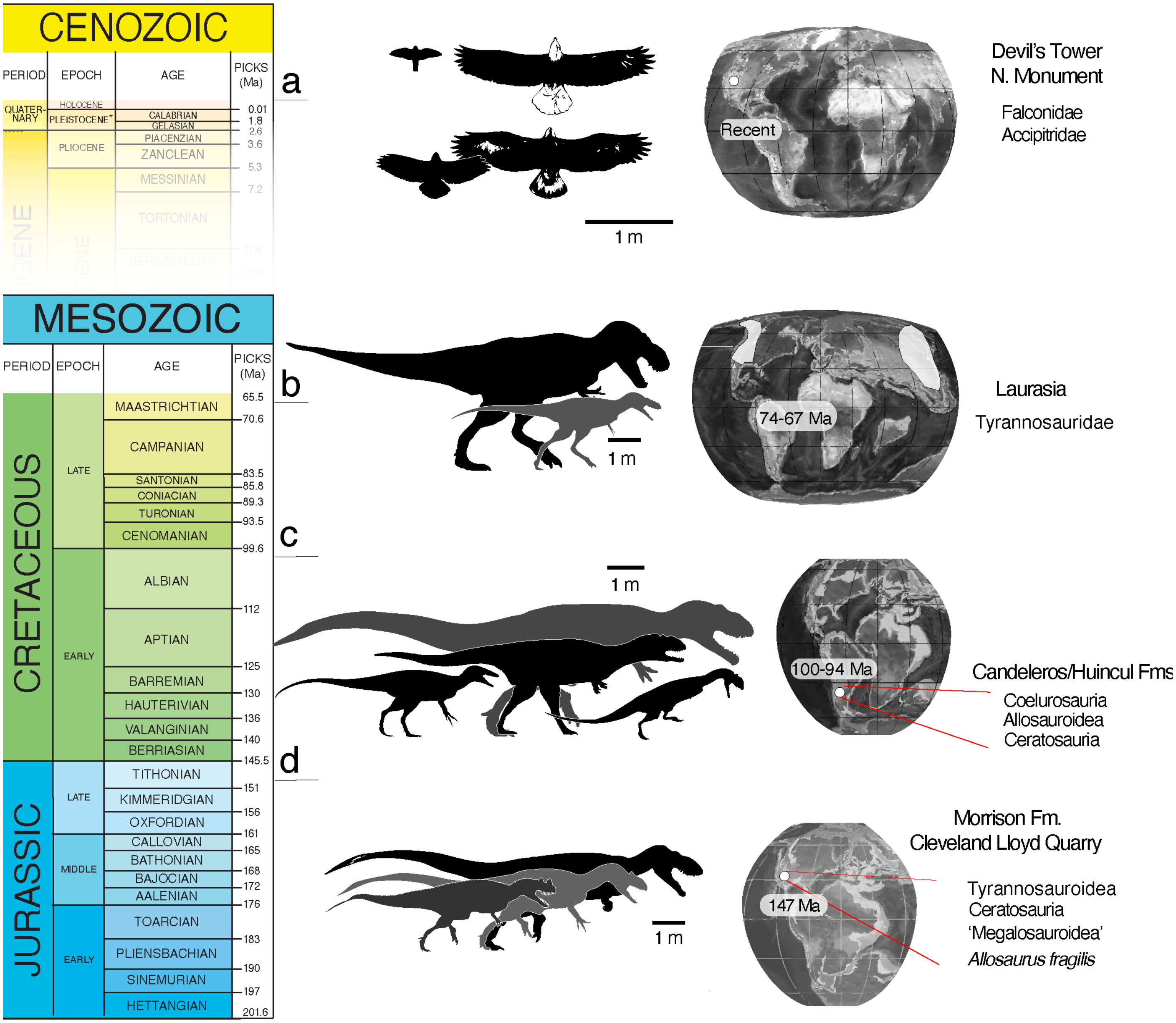

Figure 10. Campanian and Maastrichtian tyrannosaurids are the only large, toothed theropods of continental Laurasia. In contrast, theropods of other times and regions are more phylogenetically diverse, within single formations and even individual quarries. a, extant diurnal carnivorous theropods of two clades common at Devil's Tower National Monument, Wyoming, USA; b, derived tyrannosauroids are the only large theropods in eastern Asia, Laramidia, and Appalachia; c, giant allosauroids, large megaraptorans, and abelisaurid ceratosaurs span the Candaleros and Huincul Formations of Argentina; d, *Ceratosaurus*, *Allosaurus* (predominantly), megalosauroid, and tyrannosauroid fossils occur in the Cleveland Lloyd Quarry of the Morrison Formation.

to sample the AMNH *Coelophysis* specimen, we thank Carl Mehling and Mark Norell. Saebyul Choe, Beth Goldoff, and Denton Ebel provided access and assistance with thin-sectioning equipment at AMNH. We thank Thomas Carr for discussions and images of *Daspletosaurus*. We thank the Currie and Koppelhus labs for support, discussion, and motivation. For funding and support we thank Alberta Ingenuity, Canada Foundation for Innovation, National Science Foundation, Dinosaur Research Institute, a University of Alberta QEII scholarship, a Richard Gilder Graduate School Fellowship, the University of Wisconsin La Crosse, and Oklahoma State University Center for Health Sciences.

Author contributions

L.A.S. conceived the research and carried it out with M.B. and D.E.B. All authors co-wrote and/or edited iterations of the paper. L.A.S interpreted macro- (osteological) and microscopic (SEM analysis; enthesis) morphology. M.B.

and D.E.B. contributed histological and micro-CT analysis and interpretation, and A.P.R. prepared and contributed extant material for comparisons, from previous research. L.A.S, M.B., E.S., L.M.W., D.E.B., and T.R.H. wrote the manuscript, and P.J.C. provided facilities.

LITERATURE CITED

Apostolakos J., T.J. Durant. C.R. Dwyer, R.P. Russell, J.H. Weinreb, F. Alaee, K. Beitzel, M.B. McCarthy, M.P. Cote, and A.D. Mazzocca. 2014. The enthesis: a review of the tendon-to-bone insertion. Muscles Ligaments Tendons Journal 4:333–342.

Bates, K.T., and P.L. Falkingham. 2012. Estimating maximum bite force in *Tyrannosaurus rex* using multi-body dynamics. Biology Letters 8:660–664.

Bates K.T, and P.L. Falkingham. 2018. The importance of muscle architecture in biomechanical reconstructions of extinct animals: a case study using *Tyrannosaurus rex*. Journal of Anatomy 233:625–635.

Benjamin, M., T. Kumai, S. Milz, B.M. Boszczyk, A.A. Boscczyk, and J.R. Ralphs. 2002. The skeletal attachment of tendons – tendon 'entheses'. Comparative Biochemistry and Physiology Part A: Molecular & Integrative Physiology 133:931–945.

Biewener, A.A. 2005. Review: biomechanical consequences of scaling. Journal of Experimental Biology 208:1665–1676.

Bronzatti, M., R.B.J. Benson, S.W. Evers, M.D. Ezcurra, S.F. Cabreira, J. Choiniere, K.N. Dollman, A. Paulina-Carabajal, V.J. Badermacher, L. Roberto-da Silva, G. Sobral, M.R. Stocker, L.M. Witmer, M.C. Langer, and S.J. Nesbitt. 2021. Deep evolutionary diversification of semicircular canals in archosaurs. Current Biology 31:1–10.

Brown, C.M., A.P. Russell, and M.J. Ryan. 2009. Pattern and transition of surficial bone texture of the centrosaurine frill and their ontogenetic and taxonomic implications. Journal of Vertebrate Paleontology 29:132–141.

Brusatte, S.L., M.A Norell, T.D. Carr, G.M. Erickson, J.R. Hutchinson, A.M. Balanoff, G.S. Bever, J.N Choinere, P.J. Makovicky, and X. Xu. Tyrannosaur paleobiology: new research on ancient exemplar organisms. Science 329:1481–1485.

Bryant, H.N., and A.P. Russell. 1992. The role of phylogenetic analysis in the inference of unpreserved attributes of extinct taxa. Philosophical Transactions of the Royal Society of London B 337:405–418.

Carrano, M.T. 1998. What, if anything, is a cursor? Categories versus continua for determining locomotor habit in mammals and dinosaurs. Journal of Zoology, London 247:29–42.

Carrier, D.R., R.M. Walter, and D.V. Lee. 2001. Influence of rotational inertia on turning performance of theropod dinosaurs: clues from humans with increased rotational inertia. Journal of Experimental Biology 204:3917–3926.

Carter, D.R., and G.S. Beaupré. 2001. Skeletal tissue histomorphology and mechanics; pp. 31–52 in D.R. Carter and G.S. Beaupré (eds.), Skeletal Function and Form: Mechanobiology of Skeletal Development, Aging, and Regeneration. Cambridge University Press, Cambridge, U.K.

Colbert, E.H. 1989. The Triassic dinosaur *Coelophysis*. Museum of Northern Arizona Bulletin. 57:1–160.

Coombs, W.P. Jr. 1978. Theoretical aspects of cursorial adaptations in dinosaurs. The Quarterly Review of Biology 53:393–418.

Cost, I. N., K.M. Middleton, K.C. Sellers, M.S. Echols, L.M. Witmer, J.L. Davis, and C.M. Holliday. 2019. Palatal biomechanics and its significance for cranial kinesis in *Tyrannosaurus rex*. The Anatomical Record 303:999–1017.

Cox, P.G., and N. Jeffery. 2010. Semicircular canals and agility: the influence of size and shape measures. Journal of Anatomy 216:37–47.

Cullen, T.M., D.C. Evans, M.J. Ryan, P.J. Currie, and Y. Kobayashi. 2014. Osteohistological variation in growth marks and osteocyte lacunar density in a theropod dinosaur (Coelurosauria: Ornithomimidae). BMC Evolutionary Biology 14:231.

Dececchi, T.A., A.M. Mloszewska, T.R. Holtz, Jr., M.B. Habib, and H.C.E. Larsson. 2020. The fast and the frugal: Divergent locomotory strategies drive limb lengthening in theropod dinosaurs. PLoS ONE 15(5): e0223698. https://doi.org/10.1371/journal. pone.0223698

Ely, E.R., C.S Avella, J.S. Price, R.K.W Smith, J.L.N Wood, and K.L.P Verheyen. 2009. Descriptive epidemiology of fracture, tendon and suspensory ligament injuries in National Hunt racehorses in training. Equine Veterinary Journal 41:372–378.

Erickson, G.M., P.J. Makovicky, P.J. Currie, M.A. Norell, S.A. Yerby, and C.A. Brochu. 2004. Gigantism and comparative life-history parameters of tyrannosaurid dinosaurs. Nature 430:772–778.

Erickson, G.M., S.D. Van Kirk, J. Su, M.E. Levenston., W.E. Caler, and D.R. Carter. 1996. Bite-force estimation for *Tyrannosaurus rex* from tooth-marked bones. Nature 382:706–708.

Erickson, G.M., K.C. Rogers, D.J. Varricchio, M.A. Norell, and X. Xu. 2007. Growth patterns in brooding dinosaurs reveals the timing of sexual maturity in non-avian dinosaurs and genesis of the avian condition. Biology Letters 3:558–561.

Ezcurra, M.D. 2017. A new early coelophysoid neotheropod from the Late Triassic of northwestern Argentina. Ameghiniana 54:506–538.

Farlow, J.O., and T.R. Holtz, Jr. 2002. The fossil record of predation in dinosaurs; pp. 251–266 in M. Kowalewski and P.H. Kelley (eds.), The Fossil Record of Predation (The Paleontological Society Papers, Volume 8. Cambridge University Press, Cambridge, U.K.

Funston, G., P. Currie, and M. Burns. 2016. New elmisaurine specimens from North America and their relationship to the Mongolian *Elmisaurus rarus*. Acta Palaeontologica Polonica 61:159–173.

Gignac, P.M., and G.M. Erickson. 2017. The biomechanics behind extreme osteophagy in *Tyrannosaurus rex*. Scientific Reports 7:2012

Hadziselimovic, H., and L.J. Savkovic. 1964. Appearance of semicircular canals in birds in relation to mode of life. Acta Anatomica 57:306–315.

Henderson, D.M., and E. Snively. 2003. *Tyrannosaurus* en pointe: allometry minimized rotational inertia of large carnivorous dinosaurs. Proceedings of the Royal Society of London, Biology Letters 271:S57–S60.

Holtz, T.R., Jr. 2021. Theropod guild structure and the tyrannosaurid niche assimilation hypothesis: implications for predatory dinosaur macroecology and ontogeny in later Late Cretaceous Asiamerica. Canadian Journal of Earth Sciences 58:778–795.

Holtz, T.R., Jr. 2004. Taxonomic diversity, morphological disparity, and guild structure in theropod carnivore communities: implications for paleoecology and life history strategies in tyrant dinosaurs. Journal of Vertebrate Paleontology 24(Suppl. 3):72A.

Holtz, T.R., Jr. 2002. Theropod predation: evidence and ecomorphology; pp. 325–340 in P.H. Kelly, M. Koweleski and T.A. Hansen (eds.), Predator–Prey Interactions in the Fossil Record. Topics in Geobiology 17. Kluwer/Plenum, New York.

Holtz, T.R., Jr. 2001. Arctometatarsalia revisited: the problem of homoplasy in reconstructing theropod phylogeny; pp. 99–121 in J. Gauthier and L.F. Gall (eds.), New Perspectives on the Origin and Early Evolution of Birds: Proceedings of the International Symposium in Honor of John H. Ostrom. Yale University Press, New Haven, CT.

Holtz, T.R., Jr. 1995. The arctometatarsalian pes, an unusual structure of the metatarsus of Cretaceous Theropoda (Dinosauria: Saurischia). Journal of Vertebrate Paleontology 14:480–519.

Hone, D.W.E., K. Wang, C. Sullivan, X. Zhao, S. Chen, D. Li, S. Ji, Q. Ji, and X. Xu. 2011. A new, large tyrannosaurine theropod from the Upper Cretaceous of China. Cretaceous Research 32:495–503.

Hurum, J.H., and K. Sabath. 2003. Giant theropod dinosaurs from Asia and North America: skulls of *Tarbosaurus bataar* and *Tyrannosaurus rex* compared. Acta Palaeontologica Polonica 48:161–190.

Hutchinson, J.R, K.T. Bates, J. Molnar, V. Allen, and P.J. Makovicky. 2011. A computational analysis of limb and body dimensions in *Tyrannosaurus rex* with implications for locomotion, ontogeny, and growth. PloS One 6(1):e26037.

Li, D., M.S. Norell, K.Q. Gao, N.D. Smith, and P.J. Makovicky. 2010. A longirostrine tyrannosauroid from the Early Cretaceous of China. Proceedings of the Royal Society B: Biological Sciences 277:183–190.

Money, K.E., J.P. Londolt, M.J. Correia, and J. Laufer. 1974. Anatomical and physiological investigations of the vestibular system of birds. Brain, Behavior, and Evolution 10:212–227.

More, H.L., J.R. Hutchinson, D.F. Collins, D.J. Weber, S.K.H. Aung, and J.M. Donelan. 2010. Scaling of sensorimotor control in terrestrial mammals. Proceedings of the Royal Society B 277:3563–3568.

Nesbitt, S.J., R.K. Denton, M.A. Loewen, S.L. Brusatte, N.D. Smith, A.H. Turner, J.I. Kirkland, A.T. McDonald, and D.G. Wolfe. 2019. A mid-Cretaceous tyrannosauroid and the origin of North American end-Cretaceous dinosaur assemblages. Nature Ecology and Evolution 3:892–899. https://doi.org/10.1038/s41559-019-0888-0

Paul, G.S. 2005. Body and tail posture in theropod dinosaurs; pp. 238–246 in K. Carpenter (ed.), The Carnivorous Dinosaurs. Indiana University Press, Bloomington, ID.

Petermann, H., and P.M. Sander. 2013. Histological evidence for muscle insertion in extant amniote femora: implications for muscle reconstruction in fossils. Journal of Anatomy 222:419–436.

Qin, Z.-C., Q. Zhao, and X. Xu. 2019. Metatarsal II osteohistology of *Xixianykus zhangi* (Theropoda: Alvarezsauria) and its implications for the development of the arctometatarsalian pes. Vertebrata PalAsiatica 57:205–213.

Rayfield, E.J. 2004. Cranial mechanics and feeding in *Tyrannosaurus rex*. Proceedings of the Royal Society of London, Series B 271:1451–1459.

Rinehart, L.F., S.G. Lucas, A.B. Heckert, J.A. Spielmann, and M.D. Celeskey. 2009. The paleobiology of *Coelophysis bauri* (Cope) from the Upper Triassic (Apachean) Whitaker quarry, New Mexico, with detailed analysis of a single quarry block. New Mexico Museum of Natural History and Science Bulletin 45:1–260.

Sampson, S.D., and L.M. Witmer 2007. Craniofacial anatomy of *Majungasaurus crenatissimus* (Theropoda: Abelisauridae) from the Late Cretaceous of Madagascar. Society of Vertebrate Paleontology Memoir 8, Journal of Vertebrate Paleontology 27(Suppl. 2):32–102.

Sellés, A.G., B. Vila, S.L. Brusatte, P.J. Currie, and À. Galobart. 2021. A fast-growing basal troodontid (Dinosauria: Theropoda) from the latest Cretaceous of Europe. Scientific Reports 11:4855.

Schroeder, K., S.K. Lyons, and F.A. Smith. 2021. The influence of juvenile dinosaurs on community structure and diversity. Science 371:941–944.

Sereno, P.C., L. Tan, S.L. Brusatte, H.J. Kriegstein, X. Zhao, and K. Cloward. 2009. Tyrannosaurid skeletal design first evolved at small body size. Science 326:418–422.

Shaw, H.M., and M. Benjamin. 2007. Structure-function relationships of entheses in relation to mechanical load and exercise. Scandinavian Journal of Medicine & Science in Sports 17:303–315.

Shychoski, L. 2006. A geometric morphometric and finite element analysis investigating tyrannosauroid phylogeny and ontogeny emphasizing the biomechanical implications of scale. MSc thesis, University of Bristol. 125 pp.

Snively E., and A.P. Russell. 2007. Craniocervical feeding dynamics of *Tyrannosaurus rex*. Paleobiology 33:610–638.

Snively, E., and A.P. Russell. 2003. Kinematic model of tyrannosaurid (Dinosauria: Theropoda) arctometatarsus function. Journal of Morphology 255:215–227.

Snively, E., and A.P. Russell. 2002. The tyrannosaurid metatarsus: bone strain and inferred ligament function. Senckenbergiana Lethaea 82:35–42.

Snively, E., H. O'Brien, D.M. Henderson, H. Mallison, L.A. Surring, M.E. Burns, T.R. Holtz Jr, A.P. Russell, L.M. Witmer, P.J. Currie, S.A. Hartman, and J.R. Cotton. 2019. Lower rotational inertia and larger leg muscles indicate more rapid turns in tyrannosaurids than in other large theropods. PeerJ 7:e6432.

Snively, E., D.M. Henderson, and D.S. Phillips. 2006. Fused and vaulted nasals of tyrannosaurid dinosaurs: implications for cranial strength and feeding mechanics. Acta Palaeontologica Polonica 51:435–454.

Snively, E, A.P. Russell, and G.L. Powell. 2004. Evolutionary morphology of the coelurosaurian arctometatarsus: descriptive, morphometric, and phylogenetic approaches. Zoological Journal of the Linnean Society 142:525–553.

Spoor, F., T. Garland Jr., G. Krovitz, T.M. Ryan, M.T. Silcox, and A. Walker. 2007. The primate semicircular canal system and locomotion. Proceedings of the National Academy of Sciences 104:10808–10812.

Stein, K., and M. Sander. 2009. Histological core drilling: a less destructive method for studying bone histology; pp 69–80 in M.A. Brown, J.F. Kane, and W.G. Parker (eds.), Methods in Fossil Preparation. Proceedings of the first annual fossil preparation and collections symposium. Petrified Forest National Park, Arizona.

Therrien, F., and D.M. Henderson. 2007. My theropod is bigger than yours… or not: estimating body size from skull length in theropods. Journal of Vertebrate Paleontology 27:108–115.

Tumarkin-Deratzian, A.R. 2009. Evaluation of long bone surface textures as ontogenetic indicators in centrosaurine ceratopsids. The Anatomical Record: Advances in Integrative Anatomy and Evolutionary Biology 292:1485–1500

Tumarkin-Deratzian, A.R., D.R. Vann, and P. Dodson. 2007. Growth and textural ageing in long bones of the American alligator *Alligator mississippiensis* (Crocodylia: Alligatoridae). Zoological Journal of the Linnean Society 150:1–39.

Tykoski, R.S. 2005. Anatomy, ontogeny, and phylogeny of coelophysoid theropods. PhD dissertation, University of Texas at Austin, Austin, Texas, 553 pp.

Varricchio, D.J. 1993. Bone microstructure of the Upper Cretaceous theropod dinosaur *Troodon formosus*. Journal of Vertebrate Paleontology 13:99–104.

Watanabe, A., G.M. Erickson, and P.S. Druckenmiller. 2013. An ornithomimosaurian from the Upper Cretaceous Prince Creek Formation of Alaska. Journal of Vertebrate Paleontology 33:1169–1175.

White, M.A. 2009. The subarctometatarsus: intermediate metatarsus architecture demonstrating the evolution of the arctometatarsus and advanced agility in theropod dinosaurs. Alcheringa 33:1–21.

Wilson, M.C., and P.J. Currie. 1985. *Stenonychosaurus inequalis* (Saurischia: Theropoda) from the Judith River (Oldman) Formation of Alberta – new findings on metatarsal structure. Canadian Journal of Earth Sciences 22:1813–1817.

Witmer, L.M. 1995. The extant phylogenetic bracket and the importance of reconstructing soft tissues in fossils; pp. 19–33 in J.J. Thomason (ed.), Functional Morphology in Vertebrate Paleontology. Cambridge University Press, Cambridge.

Witmer, L.M., and R.C. Ridgely. 2009. New insights into the brain, braincase, and ear region of tyrannosaurs (Dinosauria, Theropoda), with implications for sensory organization and behavior. The Anatomical Record: Advances in Integrative Anatomy and Evolutionary 292:1266–1296.

Witmer, L.M., R.C. Ridgely, D.L. Dufeau, and M.C. Semones M.C. 2008. Using CT to peer into the past: 3D visualization of the brain and ear regions of birds, crocodiles, and nonavian dinosaurs; pp. 67–87 in E. Endo and R. Frey (eds.), Anatomical Imaging: Towards a New Morphology. Springer Science & Business Media, Berlin.

Yun, C. 2021.A juvenile metatarsal of cf. *Daspletosaurus torosus*: implications for ontogeny in tyrannosaurid theropods. Acta Paleontologica Romaniae 17:15–22.

Zanno, L., R.T. Tucker, A. Canoville, H.V. Avrahami, T.A. Gates, and P.J. Makovicky. 2019. Diminutive fleet-footed tyrannosauroid narrows the 70-million-year gap in the North American fossil record. Communications Biology 2:64. https://doi.org/10.1038/s42003-019-0308-7